HOLOGRAPHIC SUBSURFACE IMAGING RADAR FOR APPLICATIONS IN CIVIL ENGINEERING

A.V. Zhuravlev*, S.I. Ivashov*, V.V. Razevig*, I.A. Vasiliev*, A.S. Türk, and A. Kizilay****

*Bauman Moscow State Technical University, Russia, azhuravlev@rslab.ru
**Yildiz Technical University, Turkey

Abstract

There is increasing demand in civil engineering to get high resolution images of shallowly buried objects such as steel reinforcements, power and communication lines, pipes, etc. The described in the article radar system employing continuous wave signals was designed to obtain plan view high resolution images at shallow depths. The plan view resolution is achieved by synthetic aperture, which is formed by regular manual scanning. The current design of the system has depth resolution defined by depth of focus rather than by bandwidth. Two narrowband prototypes of the system around 7 and 14 GHz were designed. The estimated resolution of the system in the presented experiments was estimated 2 and 1.5 cm at 7 and 14 GHz respectively. The paper outlines hardware, user and embedded software, hologram reconstruction technique, and selected experimental results.

Keywords: Microwave holography, subsurface radar, non-destructive testing, imaging radar.

1 Introduction

The problem of maping shallowly buried objects arises frequently in civil engineering. Among typical objects of interest can be reinforcement bars, power and communication cables, pipes, voids, unexpected foreign objects, etc. The majority of radars available on the market for that purpose belong to impulse radars. They emit short pulses and record their return time and amplitude after reflection. As opposed to that, the holographic radar records phase and amplitude on a set of operating frequencies. Continuous wave radars in the problem of imaging shallowly buried objects can be advantageous over impulse radars for the following reasons. For a buried object at a close distance to the surface the continuous wave radar does not give multiple reverberations. The presence of a strong reflector in the vicinity to the surface presents no problem to the continuous wave radar as long as the increased level of the signal stays in the dynamic range of the system. Interpretation of obtained images of buried objects is easier due to their resemblance to respective optical images [1, 2].

In this paper a new modification of the holographic radar RASCAN [3] is presented. Both hardware implementation and signal processing technique are outlined. The paper ends with experimentally obtained images of shallowly buried objects and suggests further improvements to the system.

2 Hardware implementation

Figure 1 shows the functional block diagram of the radar. The transmitter consists of a frequency synthesizer that drives a voltage-controlled oscillator. The reference frequency of the synthesizer is provided by a quartz oscillator operating at 20 MHz. A directional coupler is used at the output of VCO to feed the local oscillator input of the mixer.

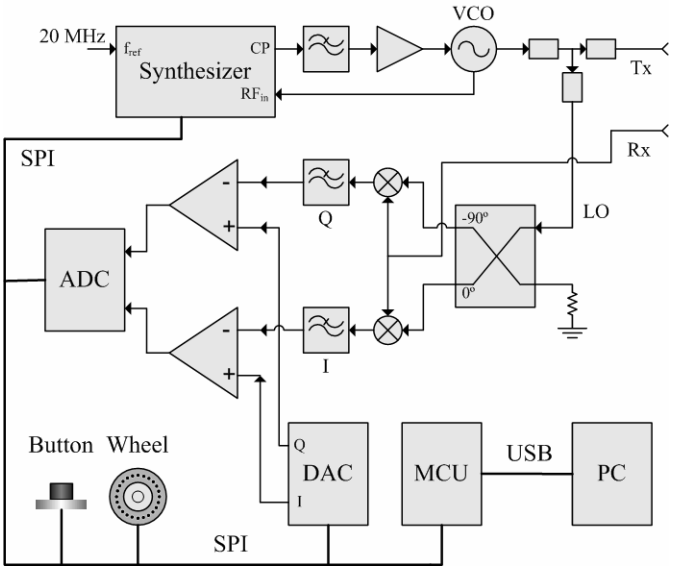

Figure 1: Principal block-diagram of the radar.

The outputs of the mixers are low pass filtered and directed to the amplifiers whose purpose is to compensate for a strong reflection by the surface. This compensation is required to keep ADC input voltage in the middle of its input range when switching among frequencies and operating over different surfaces. A microcontroller unit is used to control peripheral units such as the synthesizer, ADC, DAC, button, and marching wheel over the Serial Peripheral Interface (SPI) bus. The button serves to mark the beginning of a new scan line while the distance along a scan line is measured by the marching wheel. The microcontroller itself is connected to a PC over USB for receiving control commands and responding with packets of data or a data stream.

The radar system mounted in a housing is shown in Figure 2.

Figure 2: Radar head and control unit.

The radar head seen in the picture on the left includes all high frequency components and connects to the square control unit on the right by a cable with address and data buses as well as power supply.

3 Embedded and user software

Embedded software is responsible for peripheral units control and can run a series of tasks such as line acquisition, streaming mode operation, calibration procedure, and setup. A task is invoked by receiving a dedicated command with optional parameters from PC. Upon receiving a control command, MCU responds with a packet of data or infinitely streams the data.

At the initial power up before operation, MCU unit should be setup to work with particular type of radar head, two types of which are available at present with frequency ranges 6.4–7.0 GHz and 14.0–15.0 GHz. The setup procedure is different for two mentioned radar heads in the aspect that they need different register values for the frequency synthesizers. The values are stored at the PC-side software so that a single control unit can operate with both scanning head.

Upon power up, the calibration procedure should run to assure that the received signal stays within ADC dynamic range. For that purpose the radar head should be placed over the scan area and calibration command should be issued. At calibration, MCU drives two DAC channels to get ADC outputs to be close to the middle of ADC operational range. This is done iteratively for the full set of operational frequencies. As the result of calibration, an array of ADC values, two for each operating frequency, is obtained and stored. From this on, a pair of calibration values is used to set DAC outputs whenever the radar switches to that frequency: at image acquisition or data streaming. The calibration can be done in any desired moment whether the results of previous calibration were not satisfactory or one needs to operate on a different surface.

The PC-side software provides graphical user interface required for device operation. Line-by-line data acquisition is assisted by immediate image display. Due to the fact that the focusing technique described in the following section is based on Fourier transform the software employs interactive focusing, i.e. the focusing depth is selected with a graphical control and the result is displayed immediately. When operating with the device it was proved to be useful to present streaming data at an arbitrary frequency as a strip-chart display. This view helps assessing the results of calibration and signal swing before acquisition if the radar head is moved arbitrarily along the scan area.

4 Hologram reconstruction

The result of scanning area of interest is an array of in-phase and quadrature components of the reflected signal at the operational set of preliminary defined frequencies. This signal can be viewed as an interference pattern or a complex hologram that has both amplitude and phase. If compared to optical holography the local oscillator (LO) in Figure 1 substitutes for the reference wave.

The reconstruction of a microwave hologram implements numerically the classical optical approach to hologram reconstruction where the registered hologram is illuminated by a reference wave once again to form the image of previously exposed object at a distance [4]. The only difference is the doubled wave number of the reference wave at reconstruction. A good description of the technique is given in [5]. The following relationships formalize the technique.

$$\hat{E}(k_x, k_y; 0) = \iint E^*(x, y, 0) e^{-ik_x x} e^{-ik_y y} dxdy \qquad (1)$$

$$\hat{E}(k_x, k_y; z) = \hat{E}(k_x, k_y; 0) e^{i\sqrt{(2k)^2 - k_x^2 - k_y^2}\, z} \qquad (2)$$

$$E(x, y, z) = \frac{1}{(2\pi)^2} \iint \hat{E}(k_x, k_y, z) e^{ik_x x} e^{ik_y y} dk_x dk_y \qquad (3)$$

Equation (1) gives plane wave decomposition of complex conjugate to registered interference pattern $E(x, y, 0)$ at the interface ($z = 0$). Variables x and y are coordinates in a rectangular reference frame connected to the surface. Values k_x and k_y are spatial frequencies with physical sense of wave vector projections to the coordinate axes. Propagation back to the focusing plane at z is expressed by Equation (2), which is the result of solving the Helmholz equation for complex amplitudes. Equation (3) being the inverse Fourier transform and the result of hologram reconstruction gives the distribution of sources at the depth z parallel to the surface of sounding. The equations above are obtained in a homogeneous media characterized by the wavenumber k .

4 Experimental results

To evaluate the performance of the system a series of experiments was performed. In these experiments microwave holograms of hidden objects were acquired over stacks of plaster sheets or foam concrete slabs as seen in Figure 3. A foam block had dimensions of 59.5×25×5 cm while a sheet of plaster was 124×60×1.2 cm.

Five 0.25mm thin spreading wires on a sheet of paper, two crossing fragments of steel reinforcement, and a foil-cut letters were used in these experiments as test objects.

Figure 3: Foam concrete slabs and plaster sheets used in experiments.

Photographs of the test objects with their dimensions are shown in Figure 4.

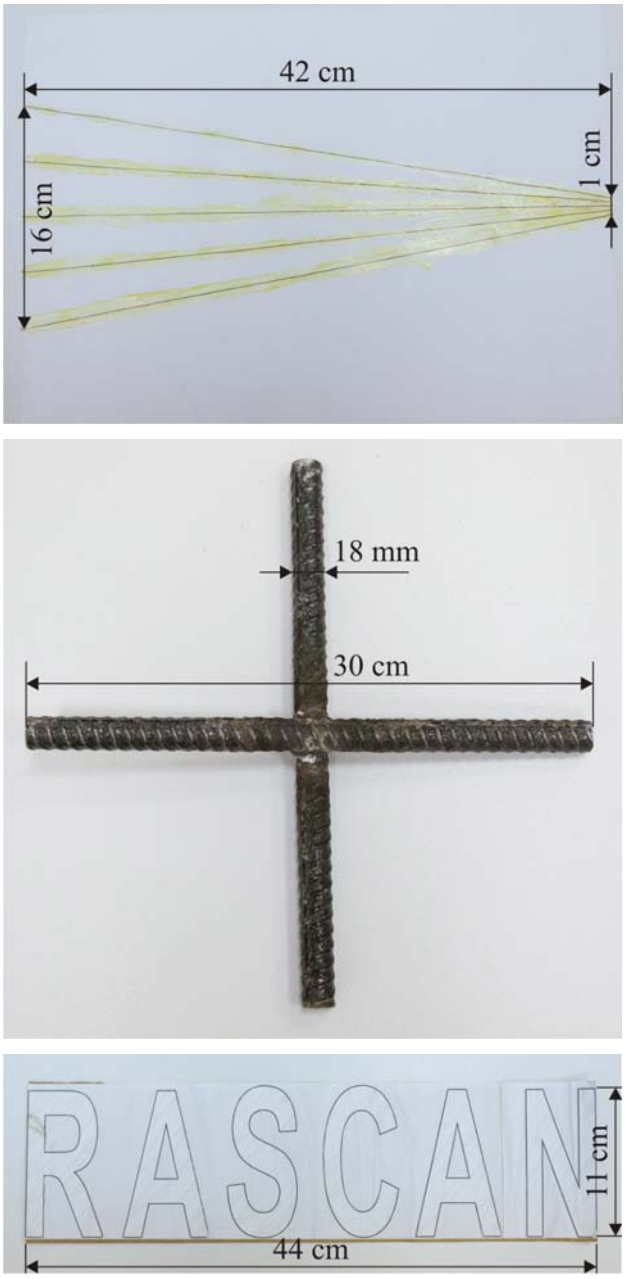

Figure 4: Test objects used in experiments.

Upon acquisition, the microwave holograms were reconstructed by the described above algorithms. The dielectric permittivity was chosen equal to 2 for foam concrete and 2.6 for plaster. The focusing depth was selected interactively to achieve best results.

Figure 5 gives registered holograms of the wires and their reconstruction at frequencies 6.6 and 13.8 GHz. The wires were placed under three plaster sheets.

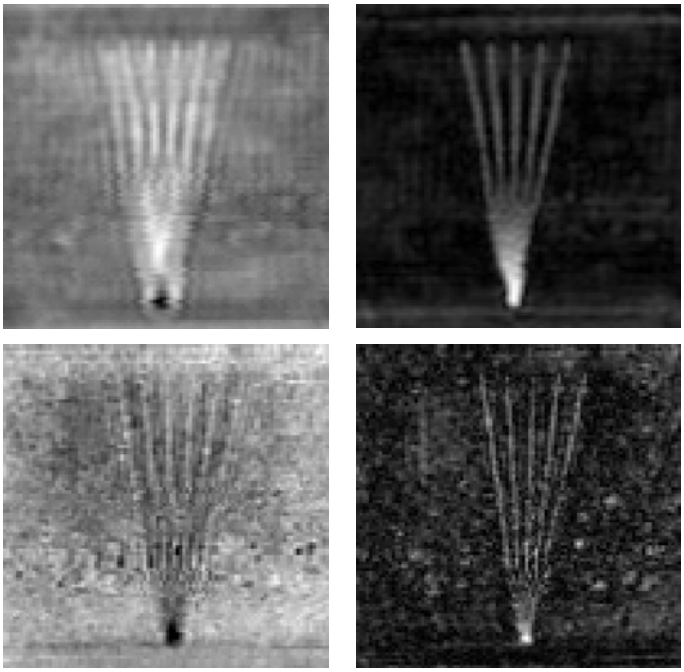

Figure 5: Thin wires under three plaster sheets at 6.6 GHz (top row) and 13.8 GHz (bottom row). Left column — holograms (in-phase components), right column — reconstruction.

Figure 5 can be used to assess plan view spatial resolution considered as the distance between two adjacent wires at the point where they separate. Such measurements give 2 cm at 6.6 GHz and 1.5 cm at 13.8 GHz. Different values are obtained when resolution is evaluated by Figure 6 where the same wires are behind five sheets of plaster. The calculated resolution for the increased depth of test object yields 2.2 cm at 6.6 GHz and 1.7 cm at 14.6 GHz. The observable deterioration of resolution is explained by increased signal extinction that limits the extent of interference pattern, or effective synthetic aperture, at reconstruction.

By comparing the images in Figure 5 corresponding to different frequencies one may remark a difference in sensitivity to small-scale irregularities in the volume of the plaster sheets. These inhomogeneities are more distinctive at a higher frequency as their size is closer to the wavelength corresponding to that frequency.

A poor result in Figure 6 at 14.6 GHz is a combination of a greater attenuation for a higher frequency as well as substantially smaller emitting power of the transmitter. Moreover, a different frequency from that of the previous experiment was chosen because observed signal amplitude is frequency dependent, especially when signal approaches to noise level.

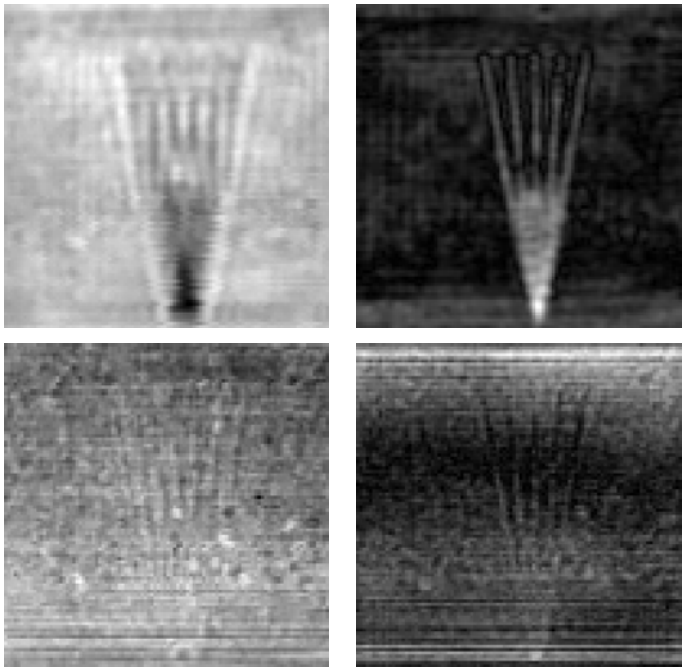

Figure 6: Thin wires under five plaster sheets at 6.6 GHz (top row) and 14.6 GHz (bottom row). Left column — holograms, right column — reconstruction.

The results obtained with the crossing reinforcement bars and foam concrete as surrounding medium are shown in Figure 7. The bars were placed in an aptly made hollow at the interface between the first and the second layers of foam concrete blocks.

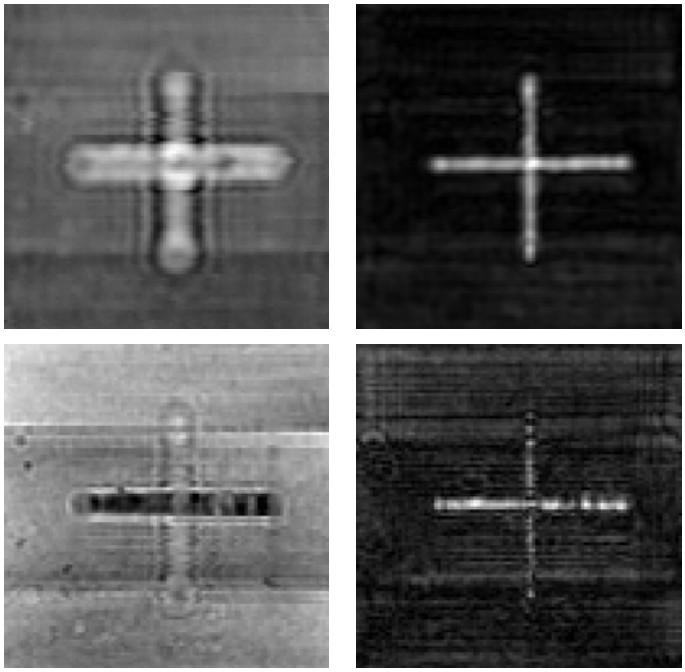

Figure 7: Crossing reinforcement bars under a foam concrete block at 6.6 GHz (top row) and 14.6 GHz (bottom row). Left column — holograms, right column — reconstruction.

The images are qualitatively similar to that of with the wires, with the width of the bars being equal to the width of the wires on the reconstructed images. This is due to the diameters both wires and bars are less than achieved plan view resolution, which at best was evaluated 2 cm at 6.6 GHz and 1.5 cm at 13.8 GHz.

The images obtained in the experiments involving foil cut letters are present in Figure 8. The letters may be considered the best reflectors of all above mentioned test objects due to their extended flat surface turned toward the radar head.

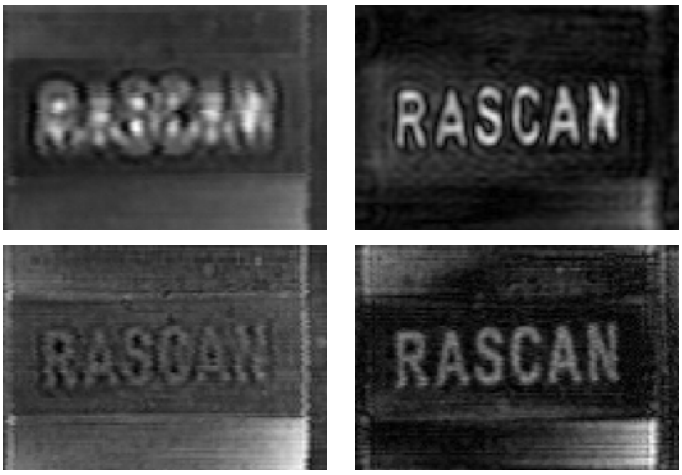

Figure 8: Foil cut letters under a foam concrete block at 6.6 GHz (top row) and 13.8 GHz (bottom row). Left column — holograms, right column — reconstruction.

Once again, the hologram at the higher frequency reveals speckles due to reflections by small irregularities. The edges of adjacent blocks to the one covering the letters are distinctive in both holograms and reconstructed images. The readable letters in the hologram at 13.8 GHz are possibly explained by more directive reflection by the letters for a shorter wavelength.

5 Conclusion and future work

The radar systems operating continuous wave signals in narrow bandwidths around 7 and 14 GHz were created and tested in typical experiments. The depth and plan view resolution are achieved in the systems by depth of focus and aperture synthesis respectively. It was shown that the plan view resolution of the system is estimated at 2 and 1.5 cm at 7 and 14 GHz respectively. The sounding frequency around 7 GHz outperforms 15 GHz in our experiments due to higher emitting power, lower attenuation in the medium, insensitivity to natural small-scale inhomogeneities of the materials, and comparable plan view resolution.

The radar system is assisted by user software that enables setup, data acquisition, and data post processing. Fourier based algorithms at reconstruction enables easy interactive focusing technique. The processed data convey shape and relative depth of buried objects and do not require special training for the operator.

The demonstrated results in clarity and resolution of reconstructed images are achieved in favourable conditions

on homogeneous construction materials. Achievable plan view resolution is sensitive to attenuation in the medium which limits the size of synthetic aperture. A clear background or isolation of buried objects is also of importance for obtaining good reconstruction.

The system can be further improved by extending its frequency bandwidth. A wider bandwidth will result in a shorter focusing depth for a buried object. The demonstrated results were obtained with focusing on only one sounding frequency with the depth of focus defined by the size of synthetic aperture.

The set of operating frequencies may be advantageous to choose adaptively depending on the medium to achieve the highest signal level as it was observed that signal amplitude is frequency dependent.

In the experiments here the dielectric permittivity was selected manually to be typical to the materials. When acquiring panoramic images it is always easy to recognize the area in the image were there are no buried objects. This area can be chosen to evaluate the dielectric permittivity of the medium in an advanced radar system without additional costs and be used at reconstruction.

Acknowledgements

This work was supported by the Russian Foundation for Basic Research and the Scientific and Technological Research Council of Turkey.

References

[1] S. Ivashov, V. Razevig, I. Vasilyev, A. Zhuravlev, T. Bechtel, L. Capineri, “The Holographic Principle in Subsurface Radar Technology”, *International Symposium to Commemorate the 60th Anniversary of the Invention of Holography*, Springfield, Massachusetts USA, October 27-29, 2008, pp. 183-197.

[2] James D. Taylor, Ultrawideband Radar: Application and Design. CRC Press, 2012.

[3] Sergey I. Ivashov, Vladimir V. Razevig, Igor A. Vasiliev, Andrey V. Zhuravlev, Timothy D. Bechtel, and Lorenzo Capineri. “Holographic Subsurface Radar of RASCAN Type: Development and Applications”, *IEEE Journal of Selected Topics in Earth Observations and Remote Sensing*, Volume 4, Issue 4, pp. 763-778, 2011.

[4] J.V. Goodman, Introduction to Fourier Optics. New York: McGraw-Hill, 2005.

[5] Sheen D.M., McMakin D.L., Hall T.E., “Three-dimensional millimeter-wave imaging for concealed weapon detection,” *IEEE Trans. Microwave Theory Tech*., Volume 49, no. 9, pp. 1581–1592, Sep. 2001.